Anisotropic superconductivity of high quality FeSe$_{1-x}$ Single crystal

Chang Il Kwon, Jong Mok Ok, and Jun Sung Kim[*]

[a] *Department of Physics, Pohang University of Science and Technology, Pohang 790-784, Korea*

Abstract

We investigate the upper critical field anisotropy Γ_H and the magnetic penetration depth anisotropy Γ_λ of a high-quality FeSe$_{1-x}$ single crystal using angular dependent resistivity and torque magnetometry up to 14 T. High quality single crystals of FeSe$_{1-x}$ were successfully grown using KCl-AlCl$_3$ flux method, which shows a sharp superconducting transition at $T_C \sim 9$ K and a high residual resistivity ratio of ~ 25. We found that the anisotropy Γ_H near T_C is a factor of two larger than found in the poor-quality crystals, indicating anisotropic 3D superconductivity of FeSe$_{1-x}$. Similar to the 1111-type Fe pnictides, the anisotropies Γ_λ and Γ_H show distinct temperature dependence; Γ_H decreases but Γ_λ increases with lowering temperature. These behaviors can be attributed to multi-band superconductivity, but different from the case of MgB$_2$. Our findings suggest that the opposite temperature dependence of Γ_λ and Γ_H is the common properties of Fe-based superconductors.

Keywords: Fe based superconductor, Single crystal, Upper critical field, Penetration depth

1. INTRODUCTION

Soon after the discovery of the Fe-based high-temperature superconductor in 2008 [1], various families of Fe-based superconductors have been reported, including the so-called "1111"-type ReOFeAs (Re = La, Ce, Pr, Nd, Sm or Gd) [1-3], the "122"-type AFe$_2$As$_2$ (A=alkaline or alkaline-earth metal) [4-5], the "11"-type FeSe/FeTe [6-8], the "111"-type AFeAs (A = Li, Na, 111-type) [9], the "21322"-type Sr$_2$VO$_3$FeAs [10, 11], and so on. All these compounds share common Fe-based layers, where superconductivity is developed [12]. Among them, tetragonal β-FeSe$_{1-x}$ [6] is of particular interest because it has the simplest crystal structure and chemical composition, showing superconductivity at $T_c \sim 9$ K without chemical doping. FeSe$_{1-x}$ can therefore provide a simple model system to unveil the superconducting mechanism for Fe-based superconductors [13, 14].

So far, a lot of studies on FeSe$_{1-x}$ have been carried out including transport measurements under high magnetic fields [15] or pressure [16], and specific heat measurements [17]. However, addressing the intrinsic superconducting properties of FeSe$_{1-x}$ was hampered by the relatively-poor quality of the available single crystals. There are several impurity phases such as α-FeSe, Fe$_7$Se$_8$ and interstitial Fe found in as-grown single crystals [15, 18], which affects significantly the superconducting properties. Therefore, growing high-quality single phase FeSe$_{1-x}$ crystal has been considered as one of the important challenges. Recently, a new growth method for FeSe$_{1-x}$ single crystal at relatively low temperatures was reported using KCl-AlCl$_3$ flux [19]. Using this method, high quality single crystal without impurity phases can be obtained and

they exhibits a large residual resistivity ratio $(\text{RRR} \geq 10)$. This allows us to study intrinsic superconducting properties of FeSe$_{1-x}$.

Here we report the intrinsic superconducting anisotropy of high-quality FeSe$_{1-x}$ single crystal, *i.e.* the anisotropy of upper critical field Γ_H and magnetic penetration depth Γ_λ. These parameters provide important information on the electric structures as well as the superconducting gap. Using the angular dependent resistivity measurements, we found that the anisotropy of the upper critical field is $\Gamma_H = 3 \sim 4$ near T_C, larger than found in the previous report ($\Gamma_H = 1 \sim 2$) [15]. This indicates that FeSe$_{1-x}$ has strong intrinsic anisotropy in the effective masses, presumably due to the van-der-walls interlayer coupling. Furthermore using the angular dependent torque magnetometry, we found that the magnetic penetration depth anisotropy Γ_λ is larger than Γ_H at low temperatures. The opposite temperature dependence of Γ_H and Γ_λ resembles MgB$_2$ [20-21] and other pnictides [22-24], revealing the multi-band superconductivity in FeSe$_{1-x}$.

2. EXPERIMENTAL DETAILS

High-quality single phase tetragonal FeSe$_{1-x}$ were grown using KCl-AlCl$_3$ flux techniques as described in Ref. [19]. The powder of pure iron and the selenium were mixed with KCl and AlCl$_3$ flux and put into the pyrex tube. Sealed pyrex tube was heated to 450℃, held at about 40 days and then a furnace cooled. The highest temperature was 450 ℃ and the lowest temperature was about 380 ℃. The tetragonal-shaped single crystals were mechanically extracted from the flux and by-product. The typical crystal size of FeSe$_{1-x}$ is 700×300×10 μm^3 as shown in the inset of Fig. 1(a). The stoichiometry of Fe and Se is confirmed by
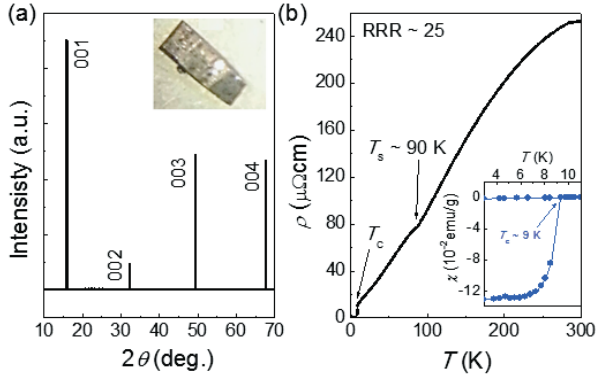
* Corresponding author: js.kim@postech.ac.kr

Fig. 1. (a) Single crystal X-ray diffraction pattern for (00*l*) peaks. Theinset shows an optical image of a FeSe$_{1-x}$ single crystal. (b) Temperature dependence of the in-plane resistivity. Magnetic susceptibility at H = 10 Oe is also shown in the inset.

energy-dispersive-X ray spectroscopy (EDS) on cleaved surface of the single crystals. The single crystal X-ray diffraction (XRD), as shown in Fig 1(a) for c-axis, revealed the good crystallinity. The conventional four-point contact resistances of FeSe$_{1-x}$ single crystals were measured in 14 T physical property measurement system (PPMS) and magnetic susceptibility was measured in 5 T magnetic property measurement system (MPMS). For torque measurements, a small single crystal, around 50×50×10 μm^3 size, was mounted onto a miniature Seiko piezo-resistive cantilever and measured in 14 T PPMS.

3. RESULTS

3.1. Characterization of FeSe$_{1-x}$ Single Crystals

The superconducting property of FeSe$_{1-x}$ single crystal was confirmed by measuring the in-plane resistivity and the magnetic susceptibility. Figure 1 (b) presents temperature dependence of the in-plain resistivity $\rho(T)$ under zero magnetic field. The resistivity $\rho(T)$ shows a sharp superconducting transition at $T_C \sim$ 9 K and a resistivity kink at ~ 90 K due to the structural transition from tetragonal to orthorhombic phases [25]. The residual resistivity ratio RRR (= ρ (300 K)/ ρ (T_c)) of FeSe$_{1-x}$ single crystal was found to be RRR ~ 25, which is much higher than the previous reports [15, 25]. The inset of Fig. 1 (b) shows the magnetic susceptibility of FeSe$_{1-x}$ single crystal at H = 10 Oe. The susceptibility $\chi(T)$ shows a clear superconducting transition at $Tc \sim$ 9 K which is consistent with the in-plane resistivity data. These results imply that the quality of FeSe$_{1-x}$ single crystals is much improved compared to those in the previous reports [15, 25].

3.2. Upper Critical Fields H_{c2} of FeSe$_{1-x}$

The upper critical field H_{c2} of FeSe$_{1-x}$ single crystal was investigated using the in-plane resistivity under high magnetic field up to 14 T. Figure 2(a) and (b) show the temperature dependence of the resistivity $\rho(T)$ curves of FeSe$_{1-x}$ at magnetic fields along the *c*-axis and the *ab*-plane, respectively. With increasing magnetic fields, the
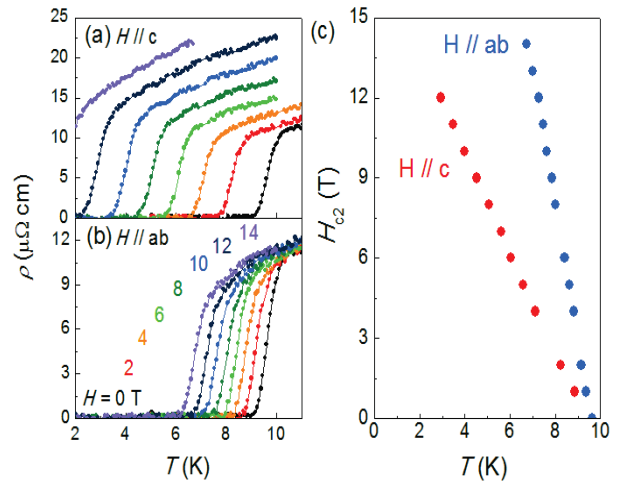

Fig. 2. Temperature dependence of the in-plane resistivity for a FeSe$_{1-x}$ single crystal under magnetic field up to 14 T for (a) H//c and (b) H//ab. (c) Upper critical fields $H_{c2}(T)$ as function of temperature for both magnetic field directions.

superconducting transition shifts to lower temperatures and becomes broader particularly for the out-of-plane field (H//c), indicating a strong anisotropy of superconductivity. Figure 2(c) shows temperature dependence of the upper critical field (H_{c2}) for both magnetic field directions. The H_{c2} values are determined by 50 % of transition in the $\rho(T)$ curves. The anisotropy parameter $\Gamma_H = H_{c2}^{ab}/H_{c2}^c = \sqrt{m_c^*/m_{ab}^*}$, where m_{ab}^* and m_c^* are the effective masses along or normal to the planes, is $\Gamma_H \sim$ 3.5 near T_C as shown in Fig 3 (c). This corresponds to the large $m_c^*/m_{ab}^* \sim$ 12, reflecting the layered structure of FeSe$_{1-x}$ with van der Waals gap.

The upper critical field (H_{c2}) near T_C changes with a slope $dH_{c2}/dT|_{T_c} \simeq$ -1.84 T/K for H//ab and $\simeq$ -5.04 T/K for H//c. The upper critical fields at zero temperature $H_{c2}(0)$ can be estimated by the Werthamer-Helfand-Hohenberg (WHH) model [26], given as $H_{c2}(0) = -0.69T_c(dH_{c2}/dT|_{TC}$. The estimated upper critical fields are $Hc2_{ab}$ = 31.3 T and H_{c2}^c = 11.4 T for both magnetic fields direction, respectively. For H//c, the WHH estimate is lower than the experimental H_{c2}^c value from the resistivity. The temperature dependence of upper critical field is in fact not described by the WHH model which is known to be applicable to a single-band dirty-limit superconductor. Therefore the multi-band electronic structures should be considered to understand the H_{c2} behaviors of FeSe$_{1-x}$. The coherence length $\xi(0)$, obtained from the $H_{c2}(0)$ values is

$$\xi_{ab}(0) = \sqrt{\frac{\phi_0}{2\pi H_{c2}^c(0)}} = 5.36 \text{ nm and } \xi_c(0) = \frac{\phi_0}{2\pi\xi_{ab}(0)H_{c2}^{ab}} =$$

1.96 nm. The *c*-axis coherence length $\xi_c(0)$ is longer than the distance between the neighbor FeAs layers (0.32nm) [4]. Therefore FeSe$_{1-x}$ should be considered as an anisotropic three-dimensional superconductor.

3.3. Upper Critical Field Anisotropy Γ_H

The more accurate anisotropy factor Γ_H for the upper critical field (H_{c2}) can be measured by the angular
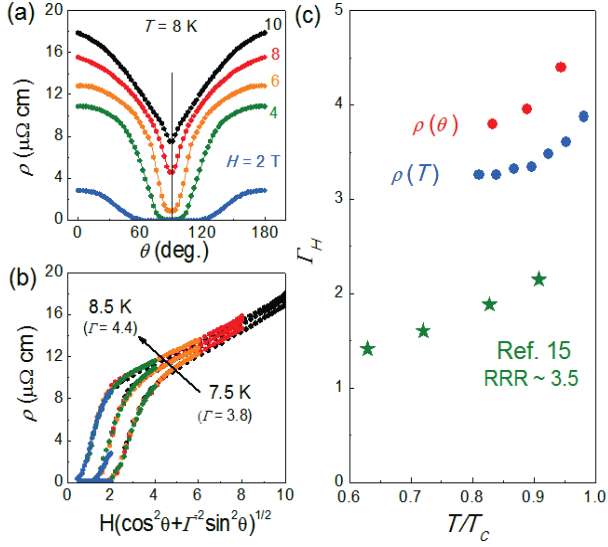
Fig. 3. (a) Angular dependence of the resistivity at 8 K with different magnetic fields of 2, 4, 6, 8, and 10 T. (b) Resistivity as a function of $\widetilde{H}$ at 7.5, 8, 8.5 K. (c) Upper critical anisotropies Γ_H estimated from the temperature dependence (blue circles) and angular dependence (red circles) of resistivity, respectively. For comparison, the data in Ref. [15] (green stars) are also plotted.

dependence of the resistivity. While the H_{c2} value determined by the resistive transition has a certain ambiguity depending on criteria, the Γ_H can be precisely determined by scaling of the angular resistivity curves using the anisotropic Ginzburg-Landau (G-L) theory [27, 28]. According to the anisotropic G-L theory, the effective upper critical field $H_{c2}^{GL}(\theta)$ is given by

$$\mathrm{H}_{c2}^{GL}(\theta) = H_{c2}^c / \sqrt{\cos^2\theta + \Gamma_H^{-2}\sin^2\theta} \; . \qquad (1)$$

Then, the resistivity curves taken at a fixed temperature but different magnetic fields are scalable with respect to $\widetilde{H} = H/H_{c2}^{GL}$, given as

$$\widetilde{H} = H\sqrt{\cos^2\theta + \Gamma_H^{-2}\sin^2\theta} \; . \qquad (2)$$

Therefore, when a correct Γ_H value is chosen, all the resistivity curves taken at different magnetic fields should collapse onto a single curve. Figure 3(a) presents the angular dependence of the resistivity at 8 K with several magnetic fields. Using these data, we obtained good scaling of the resistivity curves as shown in Fig. 3(b). The data taken at different temperatures ($T = 7.5, 8.5$ K) can also be scaled nicely as shown in Fig. 3 (b). The estimated Γ_H by the G-L model near T_C is around $\Gamma_H \sim 4.5$, somewhat larger than obtained from the resistive transition. Nevertheless, the Γ_H of our crystal is found to be almost a factor of two larger than the previous report [15].

The temperature dependencies of Γ_H estimated by two different methods are shown in the Fig. 3 (c). The Γ_H determined by the temperature and the angular dependence of the resistivity are shown with blue and red circles, respectively. In both cases, the Γ_H decreases with lowering
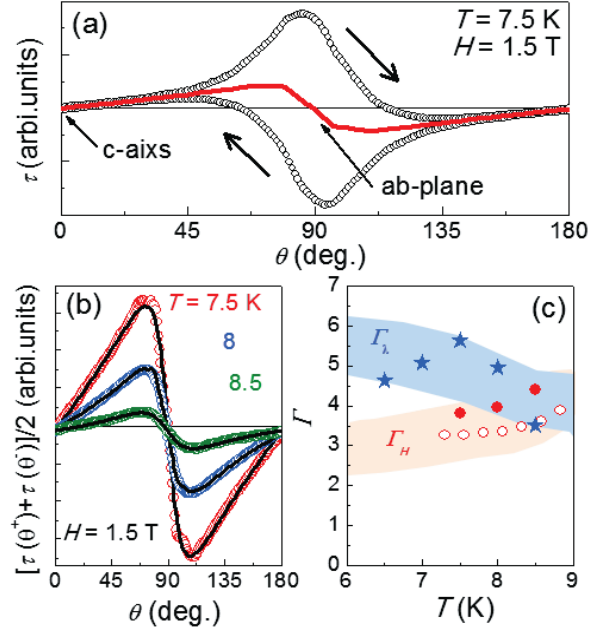
Fig. 4. (a) Angular dependence of the reversible torque data for FeSe$_{1-x}$ single crystal at several temperatures taken at a magnetic field of 1.5 T. (b) The averaged torque $(\theta) = (\tau(\theta^+) + \tau(\theta^-))/2$. The solid lines indicate fits to Eq. (4). (c) Temperature dependence of Γ_H and Γ_λ. The errors are smaller than the symbol size. The board orange/blue bands are guide to the eye.Fig. 1. (a) Single crystal X-ray diffraction pattern for (00l).

temperature. This behavior cannot be understood in terms of a single band anisotropic superconductor, which predicts the temperature independent behavior. Rather it can be attributed to the multi-band effect [29, 30]. In fact, multi-band structure of FeSe was confirmed by angle-resolved photoemission spectroscopy (ARPES) [31-33].

3.4. Penetration Depth Anisotropy Γ_λ

Multiband superconductivity is also important to understand the anisotropy of the penetration depth. In order to measure the penetration depth anisotropy (Γ_λ) of FeSe$_{1-x}$ single crystal, we carried out angular dependence of torque magnetometry. In the superconducting state, torque signal is a measure of the interaction between external magnetic field and vortices in the sample. Based on the anisotropic G-L theory, the free energy of an anisotropic superconductor in the mixed state was theoretically calculated by Kogan [34], which leads to the angle dependence of the torque signal as described by

$$\tau(\theta) = -\frac{V\phi_0 H}{16\pi\lambda_{ab}^2}\left(1 - \frac{1}{\Gamma^2}\right)\frac{\sin(2\theta)}{\epsilon(\theta)}\ln\left(\frac{\eta H_{c2}^c}{\epsilon(\theta)H}\right) \; . \qquad (3)$$

Here, V is the volume of the crystal, ϕ_0 is the flux quantum, η is a numerical parameter of the order unity, and $\epsilon(\theta) = \sqrt{\cos^2\theta + \Gamma_H^{-2}\sin^2\theta}$. As pointed out by Kogan [35], Eq. (3) considers the special case where $\Gamma = \Gamma_H = \Gamma_\lambda$. More generalized equation is shown in the Eq. (4) including two distinct anisotropies Γ_H and Γ_λ [35].

$$\tau(\theta) = -\frac{V\phi_0 H}{16\pi\lambda_{ab}^2}\left(1-\frac{1}{\Gamma^2}\right)\frac{\sin(2\theta)}{\epsilon(\theta)}\left[\ln\left(\frac{\eta H_{c2}^c}{H}\frac{4e^2\epsilon_\lambda(\theta)}{(\epsilon_\lambda(\theta)+\epsilon_H(\theta))^2}\right)-\frac{2\epsilon_\lambda(\theta)}{\epsilon_\lambda(\theta)+\epsilon_H(\theta)}\left(1+\frac{\epsilon_\lambda'(\theta)}{\epsilon_H'(\theta)}\right)\right]$$ (4)

, where the scaling function is given as $\epsilon_i(\theta) = \sqrt{\cos^2\theta + \Gamma_i^{-2}\sin^2\theta}$ and $\epsilon_i'(\theta) = \frac{d\epsilon_i(\theta)}{d\theta}$ with $i = H$ or λ.

Figure 4 (a) shows raw torque data with clockwise (θ^+) and counter-clockwise (θ^-) rotating of the magnetic field against the *c*-axis. The hysteresis originates from the vortex pinning effect. The reversible torque signals, without the vortex pinning effect, can be obtained by averaging the data taken with clockwise (θ^+) and counter-clockwise (θ^-) rotation: $\tau(\theta) = (\tau(\theta^+) + \tau(\theta^-))/2$ [22, 23]. Then, the fitting of the $\tau(\theta)$ curve to Eq. (4) yields the penetration depth anisotropy Γ_λ.

Figure 4 (b) shows the typical torque signals at 1.4 T and their fit to Eq. (4). They present good agreement with each other. The resulting temperature dependence of Γ_λ, is shown in the Fig. 4 (c). Near T_C, the Γ_λ increases with lowering temperature, but it begins to decrease near $T \sim 7$ K. It has been known that vortex pinning effects affect more significantly at low temperatures, producing large errors in the anisotropic parameter. To obtain the more accurate Γ_λ values at low temperatures, vortex-lattice shaking technique is required [23, 36]. Near T_C, however, such an effect is negligible, and we can conclude that Γ_λ is rapidly increasing with lowering temperature. This temperature dependence of Γ_λ contrasts to temperature dependence of Γ_H as shown in the Fig. 4 (c). This strongly suggests the presence of two distinct anisotropies in FeSe$_{1-x}$ as well, which is also found in other Fe-based superconductor SmFeAsO$_{1-x}$F$_x$ [22-24].

The opposite temperature dependence of Γ_H and Γ_λ have been observed in a multi-band superconductor MgB$_2$ [20-21]. What is distinct from the case of MgB$_2$ however is reversed sign of the slope of Γ_H and Γ_λ. For MgB$_2$, Γ_H increases and Γ_λ decreases with lowering temperature, opposite from the case of the FeSe$_{1-x}$ shown in Fig. 4(c). Thus, the underlying mechanism for determining Γ_H and Γ_λ seems to be quite different from the case of MgB$_2$. In fact, in MgB$_2$ there two types of Fermi surfaces (FSs) with different dimensionality, two-dimensional σ–FS with a larger superconducting gap and three-dimensional π–FS with a smaller gap. The different temperature dependence of Γ_H and Γ_λ therefore originates from different contribution of σ–FS and π–FS to the upper critical fields and the penetration depth. On the other hand, in Fe-based superconductors, both electron-type and hole-type FSs are quasi-two dimensional. Thus the difference of dimensionality between FSs is less important on the observed temperature dependence of Γ_H and Γ_λ.

In Fe-based superconductors, the Pauli limiting effects are found to be essential for the temperature dependence of Γ_H. Due to quasi-2D FSs, a slope $dH_{c2}/dT|_{T_C}$ is much larger for $H//ab$ than for $H//c$, as also found in FeSe$_{1-x}$ [Fig. 2(c)]. Thus additional Pauli limiting effects suppress H_{c2} only along the *ab*-plane at low temperatures, which reduces Γ_H at low temperatures. On the other hand, the temperature dependence of Γ_λ has only been reported for

the 1111-type *Re*FeAsO$_{1-x}$F$_x$ (*Re* = Sm, La) [22-24] remaining as an open question. Our study on FeSe$_{1-x}$ clearly demonstrates that the low-temperature enhancement of Γ_λ is the common properties of Fe-based superconductors. Strong inter-band coupling between the FSs and the multiple superconducting gaps with sign change might be important for understanding the puzzling temperature dependence of Γ_λ. Further experimental and theoretical studies on Γ_λ for other familes of Fe-based superconductors are highly desirable.

4. SUMMARY

In summary, high quality FeSe$_{1-x}$ single crystals were successfully grown by KCl-AlCl$_3$ flux methods. Using high quality single crystals showing a sharp superconducting transition at $T_C \sim 9$ K and a high residual resistivity ratio ~ 25, we found a clear evidence for two distinct anisotropies Γ_H and Γ_λ in FeSe$_{1-x}$. The large $\Gamma_H \sim 4$, near T_C is estimated from temperature and angular dependence of resistivity, which decreases with lowering temperature. In contrast, the Γ_λ shows an opposite temperature dependence. These results strongly suggest that FeSe$_{1-x}$ is a multiband superconductor, similar to MgB$_2$ and SmFeAsO$_{1-x}$F$_x$.

ACKNOWLEDGMENT

REFERENCES

[1] Y. Kamihara, T. Watanabe, M. Hirano, and H. Hosono, "Iron-based layered superconductor La[O$_{1-x}$F$_x$]FeAs (x = 0.05-0.12) with T_C=26 K," *J. Am. Chem. Soc.,* vol.130, pp. 3296-3297, 2008.

[2] X. H. Chen, T. Wu, G. Wu, R. H. Liu, H. Chen, and D. F. Fang, "Superconductivity at 43 K in SmFeAsO$_{1-x}$F$_x$," *Nature*, vol. 453, p. 761, 2008.

[3] H. H. Wen, G. Mu, L. Fang, H. Yang, and X. Zhu, "Superconductivity at 25 K in hole doped (La$_{1-x}$Sr$_x$)OFeAs," *Europhys. Lett.*, vol. 82, p. 17009, 2008.

[4] M. Rotter, M. Tegal, and D. Johrendt, "Superconductivity at 38 K in the iron arsenide (Ba$_{1-x}$K$_x$)Fe$_2$As$_2$," *Phys. Rev. Lett.*, vol. 101, p. 107006, 2008.

[5] A. S. Sefat, R. Jin, M. A. McGuire, B. C. Sales, D. J. Singh, and D. Mandrus, "Superconductivity at 22 K in Co-doped BaFe$_2$As$_2$," *Phys. Rev. Lett.*, vol. 101, p. 117004, 2008.

[6] F. -C. Hsu, J. -Y. Luo, K. W. Yeh, .T. -K. Chen T. -W. Huang, P. M. Wu, Y. -C. Lee, Y. -L. Huang, Y. -Y. Chu, D. -C. Yan, and M. -K. Wu, "Superconductivity in the PbO-type structure α-FeSe," *Proc. Natl. Acad. Sci. USA*, vol. 105, p. 14262, 2008.

[7] M. H. Fang, H. M. Pham, B. Qian, T. J. Liu, E. K. Vehstedt, Y. Liu, L. Spinu, and Z. Q. Mao, "Superconductivity close to magnetic instability in Fe(Se$_{1-x}$Te$_x$)$_{0.82}$," *Phys. Rev. B.*, vol. 78, p. 224503, 2008.

[8] G. E. Grechnev, A. S. Panfilov, V. A. Desnenko, A. V. Fedorchenko, S. L. Gnatchenko, D. A. Chareev, O. S. Volkova, and A. N. Nasiliev, "Anisotropy of magnetic properties of Fe$_{1+y}$Te," *J. Phys.: Condens. Matter*, vol. 26, p. 436003, 2014.

[9] J. H. Tapp, Z. Tang, B. Lv, K. Sasmal, B. Lorenz, P. C. W. Chu, and A. M. Guloy, "LiFeAs: an intrinsic FeAs-based superconductor with T_C = 18 K," *Phys. Rev. B.*, vol. 78, p. 060505(R), 2008.

[10] X. Zhu, F. Han, G. Mu, P. Cheng, B. Shen, B. Zeng, and H. H. Wen, "Transition of stoichiometric Sr$_2$VO$_3$FeAs to a superconducting state at 37.2 K," *Phys. Rev. B.*, vol. 79, p. 220512(R), 2008.

[11] J. M. Ok, M. J. Eom, F. Wolff-Fabris, E. Kampert, Y. J. Jo, E. S. Choi, O. A. Valenzuela, R. D. McDonald, J. H. Kim, R. K. Kremer, D. –H. Kim, C. –F. Chang, K. –T. Ko, I. I. Mazin, J. H. Shim, and J. S. Kim, "Coexistence of high-T_C superconductivity and weak ferromagnetism in natural heterostructure of iron pnictide and vanadium oxides," unpublished.

[12] M. R. Norman, "High-temperature superconductivity in the iron pnictide," *Physics*, vol. 1, p. 21, 2008.

[13] A. E. Böhmer, F. Hardy, F. Eilers, D. Ernst, P. Adelmann, P. Schweiss, T. Wolf, and C. Meingast, "Lack of coupling between superconductivity and orthorhombic distortion in stoichiometric single-crystalline FeSe," *Phys. Rev. B.*, vol. 87, p. 180505(R), 2013.

[14] Y. Mizuguchi, F. Tomioka, S. Tsuda, T. Yamaguchi, and Y. Takano, "Superconductivity at 27 K in tetragonal FeSe under high pressure," *Appl. Phys. Lett.*, vol. 93, p. 152505, 2008.

[15] S. I. Vendeneev, B. A. Piot, D. K. Maude, and V. A. Sadakov, "Temperature dependence of the upper critical field of FeSe single crystals," *Phys. Rev. B.*, vol. 87, p. 134512, 2013.

[16] S. Medvedev, T. M. McQueen, I. A. Troyan, T. Palasyuk, M. I. Eremets, R. J. Cava, S. Naghavi, F. Casper, V. Ksenofontov, G. Wortmann, and C. Felser, "Electronic and magnetic phase diagram of β-Fe$_{1.01}$Se with superconductivity at 36.7 K under pressure," *Nat. Mater.*, vol. 8, p. 630, 2009.

[17] J. –Y. Lin, Y. S. Hsieh, D. A. Chareev, A. N. Vasiliev, Y. Parsons, and H. D. Yang, "Coexistence of isotropic and extended s-wave order parameters in FeSe as revealed by low-temperature specific heat," *Phys. Rev. B.*, vol. 84, p. 220507(R), 2011.

[18] H. Okamoto, "Phase diagram evaluations," *Journal of Phase Equilibria*, vol. 12, p. 3, 1991.

[19] D. Chareev, E. Osadchii, T. Kuzmicheva, J. –Y. Lin, S. Kuzmichev, O. Volkova, and A. Vasiliev, "Single crystal growth and characterization of tetragonal FeSe$_{1-x}$ superconductors," *CrystEngComm*, vol. 15, p. 1989, 2013.

[20] V. G. Kogan, "Macroscopic anisotropy in superconductors with anisotropic gaps," *Phys. Rev. B.*, vol. 66, p. 020509(R), 2002.

[21] J. D. Fletcher, A. Carrington, O. J. Taylor, S. M. Kazakov, and J. Karpinski, "Temperature-dependent anisotropy of the penetration depth and coherence length MgB$_2$," *Phys. Rev. Lett.*, vol. 95, p. 097005, 2005.

[22] S. Weyeneth, R. Puzniak, N. D. Zhigadlo, S. Katrych, Z. Bukowski, J. Karpinski, and H. Keller, "Evidence for two distinct anisotropies in the oxypnictide superconductors SmFeAsO0.8F0.2 and NdFeAsO$_{0.8}$F$_{0.2}$," *J. Supercond. Nov. Magn.*, vol. 22, p. 347-351, 2009.

[23] S. Weyeneth, R. Puzniak, U. Mosele, N. D. Zhigadlo, S. Katrych, Z. Bukowski, J. Karpinski, S. Kohout, J. Roos, and H. Keller, "Anisotropy of superconducting single crystal SmFeAsO$_{0.8}$F$_{0.2}$ studied by torque magnetometry," *J. Supercond. Nov. Magn.*, vol. 22, p. 325-329, 2009.

[24] L. Malone, J. D. Fletcher, A. Serafin, A. Carrington, N. D. Zhigadlo, Z. Bukowski, S. Katrych, and J. Karpinski, "Magnetic penetration depth of single-crystalline SmFeAsO$_{1-x}$F$_y$," *Phys. Rev. B.*, vol. 79, p. 140501(R), 2009.

[25] R. Hu, H. Lei, M. Abykoon, E. S. Bozin, S. J. L. Billinge, J. B. Warren, T. Siegrist, and C. Petrovic, "Synthesis, crystal structure and magnetism of β-Fe$_{1.00(2)}$Se$_{1.00(3)}$ single crystals," *Phys. Rev. B.*, vol. 83, p. 224502, 2011.

[26] N. R. Werthamer, E. Helfand, and P. C. Hogenberg, "Temperature and purity dependence of the superconducting critical field, H_{c2}. III. Electron spin and spin-orbit effects," *Phys. Rev.*, vol. 147, p. 295, 1965.

[27] Z. –S. Wang, H. –Q. Luo, C. Ren, and H. H. Wen, "Upper critical field, anisotropy, and superconducting properties of Ba$_{1-x}$K$_x$Fe$_2$As$_2$ single crystals," *Phys. Rev. B.*, vol. 78, p. 140501(R), 2008.

[28] G. Blatter, V. B. Geshkenbein, and A. I. Larkin, "From isotropic to anisotropic superconductors: a scaling approach," *Phys. Rev. Lett.*, vol. 68, p. 6, 1992.

[29] Q. Han, Y. Chen, and Z. D. Wang, "A generic two-band model for unconventional superconductivity and spin-density-wave order in electron and hole doped iron-based superconductor," *Europhys. Lett.*, vol. 82, p. 37007, 2008.

[30] V. Cvetkovic, and Z. Tesanovic, "Multiband magnetism and superconductivity in Fe-based compounds," *Europhys. Lett.*, vol. 85, p. 37002, 2009.

[31] D. Liu, W. Zhan, D. Mou, J. He, Y. –B. Ou, Q. –Y. Wang, Z. Li, L. Wang. L. Zhao, S. He, Y. Peng, X. Liu, C. Chen, L. Yu, G. Liu, X. Dong, J. Zhang, C. Chen, Z. Xu, and J. Hu, "Electronic origin of high-temperature superconductivity in single-layer FeSe superconductor," *Nat. Comm.*, vol. 3, p. 931, 2012.

[32] J. Maletz, V. B. Zabolotnyy, D. B. Evtushinsky, S. Thirupathaiah, A. U. B. Wolter, L. Harnagea, A. N. Yaresko, A. N. Vasiliev, D. A. Chareev, A. E. Böhmer, F. Hardy, T. Wolf, C. Meingast, E. D. L. Rienks, B. Büchner, and S. V. Borisenko, "Unusual band renormalization in the simplest iron-based superconductor FeSe$_{1-x}$," *Phys. Rev. B.*, vol. 89, p. 220506(R), 2014.

[33] K. Nakayama, Y. Miyata, G. N. Phan, T. Sato, Y. Tanabe, T. Urata, K. Tanigaki, T. Takahashi, "Reconstruction of band structure induced by electronic nematicity in FeSe superconductor," Arxiv:1404.0857.

[34] V. G. Kogan, "London approach to anisotropic type-II superconductors," *Phys. Rev. B.*, vol. 24, p. 1572, 1981.

[35] V. G. Kogan, "Free energy and toque for superconductors with different anisotropies of H_{c2} and λ," *Phys. Rev. Lett.*, vol. 89, p. 237005, 2002.

[36] M. Willemin, C. Rossel, J. Hofer, H. Keller, A. Erb, and E. Walker, "Strong shift of the irreversibility line in high-T_C superconductors upon vortex shaking with an oscillating magnetic field," *Phys. Rev. B.*, vol. 58, p. 5940(R), 1998.